International Journal of Coal Science & Technology (2024) 11:7
https://doi.org/10.1007/s40789-023-00658-6

RESEARCH

Geochemical and petrological studies of high sulfur coal and overburden from Makum coalfield (Northeast India) towards understanding and mitigation of acid mine drainage

Angana Mahanta[1,2] · Debashis Sarmah[1] · Nilotpol Bhuyan[1] · Monikankana Saikia[1,2] · Sarat Phukan[3] · K. S. V. Subramanyam[4] · Ajit Singh[1,2] · Prasenjit Saikia[1,2] · Binoy K. Saikia[1,2]

Received: 23 September 2023 / Accepted: 31 October 2023

Abstract

Opencast coal mining produces trash of soil and rock containing various minerals, that are usually dumped nearby the abandoned sites which causes severe environmental concern including the production of acid mine drainage (AMD) through oxidation pyrite minerals. The current study entailed assessing the potential production of AMD from an opencast coal mining region in Northeast part of India. In order to have a comprehensive overview of the AMD problem in Makum coalfield, the physico-chemical, geochemical, and petrological characteristics of the coal and overburden (OB) samples collected from the Makum coalfield (Northeast India) were thoroughly investigated. The maceral compositions reveal that coal features all three groups of macerals (liptinite, vitrinite, and inertinite), with a high concentration of liptinite indicating the coal of perhydrous, thereby rendering it more reactive. Pyrite (FeS_2) oxidation kinetics were studied by conducting the aqueous leaching experiments of coal and (OB) samples to interpret the chemical weathering under controlled laboratory conditions of various temperature and time periods, and to replicate the actual mine site leaching. Inductively coupled plasma-optical emission spectroscopy (ICP-OES) was operated to detect the disposal of some precarious elements from coal and OB samples to the leachates during our controlled leaching experiment. The Rare earth element (REE) enrichment in the samples shows the anthropogenic incorporation of the REE in the coal and OB. These experiments reveal the change in conductivity, acid producing tendency, total dissolved solid(TDS), total Iron(Fe) and dissolved Sulfate(SO_4^{2-}) ions on progress of the leaching experiments. Moreover, the discharge of FeS_2 via atmospheric oxidation in laboratory condition undergoes a significant growth with the rise of temperature of the reaction systems in the environment and follows pseudo first order kinetics. A bio-remediative strategies is also reported in this paper to mitigate AMD water by employing size-segregated powdered limestone and water hyacinth plant in an indigenously developed site-specific prototype station. Apart from neutralisation of AMD water, this eco-friendly AMD remediation strategy demonstrates a reduction in PHEs concentrations in the treated AMD water.

Keywords Opencast mining · Pyrite oxidation · Coal geochemistry · Coal petrology · Rare earth elements · AMD remediation

1 Introduction

High-sulfur coal mining activities are generally associated with acid mine drainage (AMD) problem that has a great research objective in view of its effect on ecosystem as well as human health (Sun et al. 2015). AMD, a major concern for the mining industry worldwide, originates when pyrite (FeS_2) and other sulfide minerals deteriorate due to oxidation in the presence of oxygen, water, microbes (Thiobacillus thiooxidans and Thiobacillus ferrooxidans), and air (Chen et al. 2021). The Northeastern Indian coal

✉ Binoy K. Saikia
bksaikia@neist.res.in; bksaikia@gmail.com

1 Coal and Energy Division, CSIR-North East Institute of Science and Technology, Jorhat,, Assam 785006, India

2 Academy of Scientific & Innovative Research (AcSIR), Ghaziabad 201002, India

3 Department of Geological Sciences, Gauhati University, Guwahati, Assam 781014, India

4 Geochemistry Division, CSIR- National Geophysical Research Institute, Uppal Road, Hyderabad 500007, India

Published online: 03 February 2024

have high sulfur contents (2%–8% sulfur, where 75%–90% is organically bound, while the rest is in inorganic form) and a part of which is pyritic (Saikia et al. 2015a). Besides a very small percentage of pyritic sulfur, the effect of acid leachates produced in large quantities around the area by abandoned mines in the northeastern coalfield, Margherita (India) is very significant and cannot be overlooked (Saikia et al. 2015b). It can seriously impact plant development and disrupt the environment in the area (Daraz et al. 2022). In accordance with prior investigations, AMD has been correlated with elevated concentrations of various elements (such as iron, magnesium, aluminium, and some other heavy metals) and metalloids that eventually diminish pH values below 2, leads to high salinity, hardness, an extreme solubility and imparts exceptionally corrosive nature (Chabukdhara and Singh 2016; CHON et al. 1999; Dutta et al. 2020; Swer and Singh 2004). Additionally, its acidic chemical composition is extremely fragile and often modified by seasonal and tidal fluctuations (Jiao et al. 2023). The most widespread element Fe^{2+} renders up the majority of the metal ions in AMD. Fe^{2+} precipitates into iron hydroxide in water after oxidizing with dissolved oxygen, imparting the water a brownish brown appearance (Chen et al. 2021). In case, AMD releases itself right away into the surrounding waters, it will not only profoundly pollute the water body in its natural state, but will also further jeopardise the integrity of the soil's structure, trigger soil compaction, and harm the growing environment, including foliage because of incorporation of heavy metals to the earth's ground through AMD (Jiao et al. 2023). The primary species consists of FeS_2 and a number of other minerals, including pyrrhotite (Fe_xS) and galena (PbS) include sulfides. Pyrite is the most predominant sulfide mineral found in coal, is present (Du et al. 2022). The extent and pace of pyrite oxidation have a substantial effect on AMD development (Dutta et al. 2020).Pyrite oxidation in the presence of water and air due to natural processes or anthropogenic activities, leading to the formation of acid (H^+), sulfates (SO_4^{2-}), and aqueous Fe^{2+} ions

$$FeS_2 + 3.5O_2 + H_2O \longrightarrow Fe^{2+} + 2HSO_4^- \quad (1)$$

Gamut of factors like geochemistry of the governing mining site, genesis of high sulfur coal, and oxidation of pyrite are responsible for the formation of such acidic water in a coal mine area (Chabukdhara and Singh 2016). The two primary contributors of water contamination are leachate from coal and runoff water from overburden(OB) heaps (Dutta et al. 2020). According to studies on the geochemistry and nano-mineralogy of feed coals and mine overburden samples from this area, it is found that; even though pyrite itself was not detected in the samples, the existence of considerable quantities of jarosite and, in a particular case, melanterite may indicate that any pyrite that existed in those materials has deteriorated through oxidation with exposure to the atmosphere at mining site (Saikia et al. 2015b). The presence of Quartz, kaolinite, and illite as dominant crystalline mineral assemblages and a little trace of pyrite and jarosite(product of pyrite oxidation); in both coal samples of Makum coalfield as well in the OB sedimentary deposits, suggest about the detrital origin of coal. (Saikia et al. 2015b). Further, most metal ions, including very little amount of REEs, can dissolve under the low pH conditions of AMD (Li and Wu 2017). AMD in this region is attributed to the influencing factors such as presence of iron forming minerals (amorphous Fe-oxides or hydroxides) and porewaters associated with mineral matter. Reports of geochemical analysis also indicates that these factors led to the pyrite oxidation in the accompanying strata (Saikia et al. 2015b). In comparison to other waterbodies, AMD has hundreds of magnitude more of REEs and yttrium available in it and that can be used as raw materials in renewable energy sector (Ayora et al. 2016). Therefore, a thorough knowledge of AMD from its inception to remediation is very much needed and accordingly the forecastination of an ecofriendly plan for treatment by analysing the leaching behaviour of coal and OB of the Makum region can be implemented. For the purpose of remediate AMD-contaminated water and soil, an assortment of technologies and approaches have been employed. Previous studies reported that, classical AMD treatment options, for instance, include acid neutralization by supplying alkaline substances such as $CaCO_3$, NaOH, Na_2CO_3, and MgO (Daraz et al. 2022). AMD contamination is mitigated using passive methods also, that depend on natural and biological processes and incorporate anaerobic sulfate-reducing bioreactors and some unconventional organic substances etc., (Daraz et al. 2022; Villegas-Plazas et al. 2022). It exposes important research gaps, issues and opportunities (Chen et al. 2021). Regarding curing AMD, each of these modalities have pros and cons (Jiao et al. 2023). Numerous studies have been published in the literature, but they have all emphasized on one particular aspect of AMD repair (Daraz et al. 2022; Ighalo et al. 2022; Tu et al. 2022). Hence, the objectives of the current study is to comprehensively understand the mineralogy, geochemistry, petrology, and aqueous leaching behaviour of the high-sulfur coals and OB samples collected from the northeast coalfield. Herein, to investigate the fluctuation of pyritic sulfur levels in coal and OB samples, aqueous leaching of high sulfur coal and OB samples will be carried out, with respect to different time period at different temperatures and a detailed kinetics study of depyritization experiment will be conducted. From detailed literature survey on this area, we have come to know that; for optimum management technique for AMD, it is necessary

to estimate the extent of transformation and mobilization of pyrite minerals present in coals and OB. There is a dearth of knowledge on the kind, exact concentrations, mechanism of occurrence, and elemental makeup of pyrite minerals in northeast coals and OB. This study will also provide insights on the mobility of elements near the Makum coalfield based on their mode of leaching, notably REEs. The distribution and geochemistry of rare earth elements (REEs) in the samples have attracted special focus because of their significance to the economy. Despite being important on the globe as a whole, hardly a much is known about the distribution of REEs in these high-sulfur coals in the northeast. Herein, in-depth studies have been conducted on the instances, distribution, and leaching behaviour of REEs in these high-sulfur coal and OBs to fulfil existing gap in research. Preventing the formation of AMD in most mine sites is not a feasible task in many regions. Hence, we prefer to go for collecting, treating and discharging the mine water. The selection of AMD treatment options depends on the composition, pH, and costs. Many economic and environmental considerations influence the decision of which AMD remediation method to adopt. Sometimes a remediation system's real environmental cost is not immediately obvious. Considering the variable chemical composition of AMD with varying source, treatment strategy, and waste emitted during treatment processing; it doesn't seem any particular AMD processing methodology that can be implemented for all AMD. Research is currently underway to identify reasonable AMD mitigation solutions in light of the requirement to lower costs associated with treatment. Our proposed technique is very cost effective as compared to other chemical processes. In this study, we have demonstrated distinct processes to remediate AMD; one is tested in a lab, and the other is a prototype station located in a pilot plant at CSIR-NEIST, Jorhat. A prototype station with a sequential alkalinity producing technology and biological processes is designed. Thus, the comprehensive geochemical research reported in this paper will provide new avenue towards the management of acid mine drainage problem by considering the environmental impact of the AMD generation in coal mining industry through an in-depth comprehension of AMD from its genesis to remediation. This study may be relevant for large-scale deployment of these strategies to provide new routes for more sustainable AMD remediation technique during mining. A future course of action for AMD treatment can be executed in line with this current work. In general, the recommendation of our study will be valuable in directing AMD remediation and budget allocation. However, further investigation on substantial treatment methods coupled with resource recovery and recycling should be encouraged to compensate the adverse consequences of acidic effluent.

2 Materials and methods

2.1 Geology of the area, sampling pattern and collected samples

Makum coalfield is the largest coal mining area in the entire Assam-Arakan Basin (27°15' to 27°25'N latitude and 95°40' to 95°50'E longitude). The coalfield is situated in the northeastern most extension of the Patkai range in Assam (Fig. S1). Coal mining activities are also widespread in its adjoining part in Arunachal Pradesh. Although there were five mines, presently there is only one active open-cast mine is in operation at Tirap site of Margherita. This mine belongs to the North Eastern Coalfields Ltd., a subsidiary of Coal India Ltd. However, in the surrounding region of this mine there are numerous small-scale mines, that are operated by private parties. The coalfield is part the Naga Schuppen Belt of the Assam-Arakan Basin and sandwiched between two thrusts, viz., Margherita Thrust to the northeast and Disang Thrust to the southwest (Fig. S1 in the Supplementary Material). The Oligocene succession of the Tikak Parbat Formation has prominent coal bearing horizons. The Tikak Parbat Formation conformably overlies the Baragolai Formation, that constitutes the middle part of the Barail Group and unconformably overlain by the Miocene Tipam Sandstone Formation. The Tikak Parbat Formation comprises alternations of sandstone, siltstone, mudstone, shale, carbonaceous shale, clay and coal seams (Misra 1990). Altogether there are five coal seams in the coalfield. The base of the Tikak Parbat Formation is marked by a thick coal seam known as the 60ft seam in the coalfield. It is the main producing coal seam in the coalfield. There is another one large coal seam known as the '20ft seam' that overlies the '60ft seam'. These two coal seams are persistent throughout the coalfield. The thickness of the other three coal seams ranges from 3 to 8 ft. Due to intense deformation, caused by the thrusting, the coals in the Makum coalfield are highly friable. Based on random vitrinite reflectance and volatile matter content, the coals are classified between subbituminous to high volatile bituminous indicating low to medium rank nature (Singh and Singh 2001). The stratigraphic succession of Makum coalfield and the adjoining region in the Naga Schuppen Belt is given in the Fig. S1 (Mathur and Evans 1964).

For the entire study, coal and overburden samples were collected from the two active seams of 6.09 and 18.30 m at the Tirap open cast mine (colliery) in the Makum coalfield, Margherita by using standard method (ASTM, 2013). Eight coal samples were collected at different times from different locations and seam of the Makum coalfield and were designated as TpHM1, TpHM2, TpC20, TpC60, TpC5, C1, C2, and C3.

Fe-hydroxides continue to settle in AMD-contaminated waterways; therefore, samples were collected from the ochreous surface layer (2 mm) as well as the whole sediment top (30 mm). Silt samples were collected from the shallow water (< 2 feet) by plunging containers in the stream bed and scooping sediment directly into containers. Water samples were collected from the Tirap collieries coal mine water sources, as well as other sources such as rives, steams, and seepage water.

All total three overburden (OB) samples were collected and named as TpOB20, TpOB60, OB3. SE1, is the representative codes of the collected AMD water sample. Table S1 represents all the information involved in the mentioned sample codes.

2.2 Petrographic analysis

For coal petrographic analysis epoxy resin bound pellets of 0.025 m diameter were prepared from 0.001 m size coal particles and polish to a final of 5×10^{-8} m. The samples were observed under a Leica DM 6000P microscope fitted with oil immersion microscope. Fluorescence illumination using blue light excitation were utilized for observing fluorescence of macerals, especially in identification of liptinite macerals. The reflectance of vitrinite macerals was done using the photometer (MSP 200) component that was attached to the microscope via optical fibre. The ICCP system 1994 were followed for identification and classification of macerals (for Coal, 2001; ICCP, 1998; Pickel et al. 2017).

2.3 Physico-chemical analysis

2.3.1 Aqueous leaching experiments of coal and OB

The aqueous leaching experiments conducted to investigate the releasing tendency of some selected trace and heavy elements. 20 g of each finely ground coal (TpC20) and overburden (TpOB20) samples were allowed to react with distilled water (150 ml) for 30, 60, and 90, mins at a reaction temperature of 25, 45, and 90 °C, respectively at a stirring rate of 150 rpm. Table S2 represents the reaction parameters and other conditions applicable in the experiment. The supernatant liquids were filtered with a Whatmann-41 filter paper and collected for different physico-chemical and elemental analyses. Filtrates were labelled as TpC-1, TpC-2, TpC-3, TpC-4, TpC-5, TpC-6, TpC-7, TpC-8, TpC-9 and T_pOB-1, T_pOB-2, T_pOB-3, T_pOB-4, T_pOB-5, T_pOB-6, T_pOB-7, T_pOB-8, T_pOB-9, respectively depending on the reaction parameters used, which has been mentioned later in Table 1. The residues of the leached samples were also subjected to selected chemical analyses as mentioned in later part. The Fe and sulfate analysis were carried out by following the standard procedure mentioned elsewhere (Vogel 1961).

Table 1 Physical analysis of aqueous leachates of coal (TpC20) and coal (TpOB20) at different leaching times and reaction temperature

Sample code	Leaching time (min)	Reaction temperature (°C)	pH	EC (µS/cm)	DO (mg/L)	TDS (ppm)	Fe (mg/L)	SO_4^{2-} (mg/L)
Aqueous leachates of coal sample (TpC20)								
TpC-1	30	25	6.6	166	4.36	120	0.11	76.0
TpC-2	60	25	6.0	294	4.12	184.4	0.09	132.44
TpC-3	90	25	5.6	152	3.47	102.2	0.10	78.58
TpC-4	30	45	5.6	151	5.12	95.08	0.13	72.72
TpC-5	60	45	5.3	396	3.25	130.6	0.06	99.68
TpC-6	90	45	4.9	217	3.14	114.8	0.23	95.64
TpC-7	30	90	5.4	189	4.10	105.0	0.02	76.22
TpC-8	60	90	5.1	216	4.06	118.0	0.13	84.28
TpC-9	90	90	4.5	247	3.72	135.3	0.05	116.44
Aqueous leachates of overburden sample (TpOB20)								
TpOB-1	30	25	3.2	3700	3.90	3.711	11.02	2456.4
TpoB-2	60	25	3.2	4220	2.70	3.695	10.75	2972.0
TpOB-3	90	25	3.2	2910	2.65	3.810	11.06	1939.6
TpOB-4	30	45	3.2	3290	5.38	2.810	8.13	1975.4
TpOB-5	60	45	2.5	6830	4.40	2.988	9.98	1994.0
TpOB-6	90	45	2.8	6040	3.86	2.410	7.73	1885.8
TpOB-7	30	90	2.5	6930	4.01	2.921	10.60	1752.2
TpOB-8	60	90	2.4	7300	3.76	3.131	8.14	1913.4
TpOB-9	90	90	2.4	6790	3.15	2.337	7.58	1461.2

2.3.2 Physico-chemical analysis of the aqueous coal and OB leachates and residues

The aqueous leachates of the coal and OBs were subjected to pH, EC (electrical conductivity) and TDS (total dissolved solid) analysis by using a LAQUAtwin-pH-11/LAQUAtwin-EC-33/TDS meter. Fe and sulfate analysis in the leachates were analysed using standard analytical methods (Vogel 1961). The total sulfur contents in the residue samples were determined by using Leco S-144DR dual-range sulfur analyzer.

2.3.3 Kinetics of the aqueous Depyritisation

During aqueous leaching at 25, 45, and 90 °C, the residues of the coal (TpC20) and over burden (TpOB20) samples were undergone a series of reactions and the determination of pyritic sulfur contents were carried out (ASTM D2492). The kinetic parameters (rate constant, activation energy, and frequency factor) involved during the depyritisation reaction were also calculated following the previously reported method (Baruah et al. 2006).

2.4 Rare earth geochemistry of coal and OB samples

In order to get an insight to the rare earth elements (REE) present in the coal and OB samples collected from the Makum coalfield, their distributions had been investigated. The REEs analysis are ideal for studying a wide range of geochemical processes. Increasing concern about the global supply of rare earth elements (REE) as critical materials for batteries and other electronic components (Humphries 2010) has prompted the searches for additional potential sources of recycled or mineable REE (Binnemans et al. 2013). Therefore, the relative abundances of REE in such coal mine sediments/overburden and raw coals had been extensively studied to identify the competing processes governing REE fractionation in a set of samples collected from the Makum coal field.

2.5 Site-specific mitigation of AMD and prototype development

The goals of the current study are to ascertain the seasonal fluctuation of AMD in the Makum opencast mining impacted region, and the AMD remediation procedure in a sustainable way. Utilizing modern experimental instruments and laboratory-based techniques, the physico-chemical characteristics of the materials gathered are examined. By employing size-segregated powdered limestone, a straightforward laboratory-based AMD remediation procedure has been carried out in the current work. Applying an active chemical treatment to remove metals and acidity of AMD can be a costly and time-consuming procedure. In recent years, a number of passive treatment methods that do not require constant chemical inputs and instead use naturally occurring chemical and biological processes to remove polluted mine waters had been demonstrated (Martínez et al. 2019). Herein, we used some fundamental scientific solutions to help alleviate the condition. Two distinct site-specific processes had been used by us to remediate AMD, one was tested in a laboratory, and the other was a prototype station located in a pilot plant. Details of the experimental methodologies for this lab-scale and prototype-based AMD remediation study are mentioned in the supplementary document.

Methodology of different analytical characterization techniques, such as X-ray photoelectron spectroscopy (XPS), HR- High-resolution transmission electron microscopy (TEM), Inductively Coupled Plasma Optical Emission Spectrometer analysis (ICP-OES) are included in supplementary information (SI).

3 Results and discussion

3.1 Maceral composition of coal and OB

Two representative coal samples (C3 and TpH-M1) were selected for coal petrographic analysis for the present study. In few notable publications earlier (Misra 1990), coal petrographic analyses of the Makum coals had been carried out and it reported about the evidence of 20.6%–80.8% of vitrinite, 7.0%–16.2% of liptinite, 0.8%–19.8% of inertinite and 4.0%–78.6% of mineral matters in Makum coal. The Makum coal is composed of 81.7%–94.6% vitrinite, 2.6%–14.4% liptinite,0.4%–2.2% inertinite and 0.1%–9.2% mineral matter (Singh and Singh 2001). The representative samples that were being selected for the present study show maceral composition similar to that of (Misra 1990). The analysis establishes presence of all the three groups of macerals in Makum coal. The liptinite is found to be in the range of 4.4%–49.6% (Table S3). The volume percent of vitrinite group of macerals in Makum coal is found in the range from 21.2% to 24.4%, while inertinite is the least abundant group of macerals in the Makum coal (4.4%–14.8%). The vitrinite group is represented dominantly by collotelinite (Figs. 1, 2) with a minor fraction of collodetrinite (Figs. 1b, c, f, 2b). Liptinite macerals are represented by cutinite (Fig. 1a, c and e), resinite (Fig. 2a, c, d and f), sporinite (Figs. 1c, 2a, c), suberinite, liptodetrinite (Figs. 1e, 2a) and exsudatinite (Fig. 1a and e). Dominance of these liptinite macerals, thus, also indicate derivation from terrestrial plants. All the liptinite macerals show light yellow fluorescence colour indicating low rank (subbituminous) of the coal (Gogoi et al. 2020).

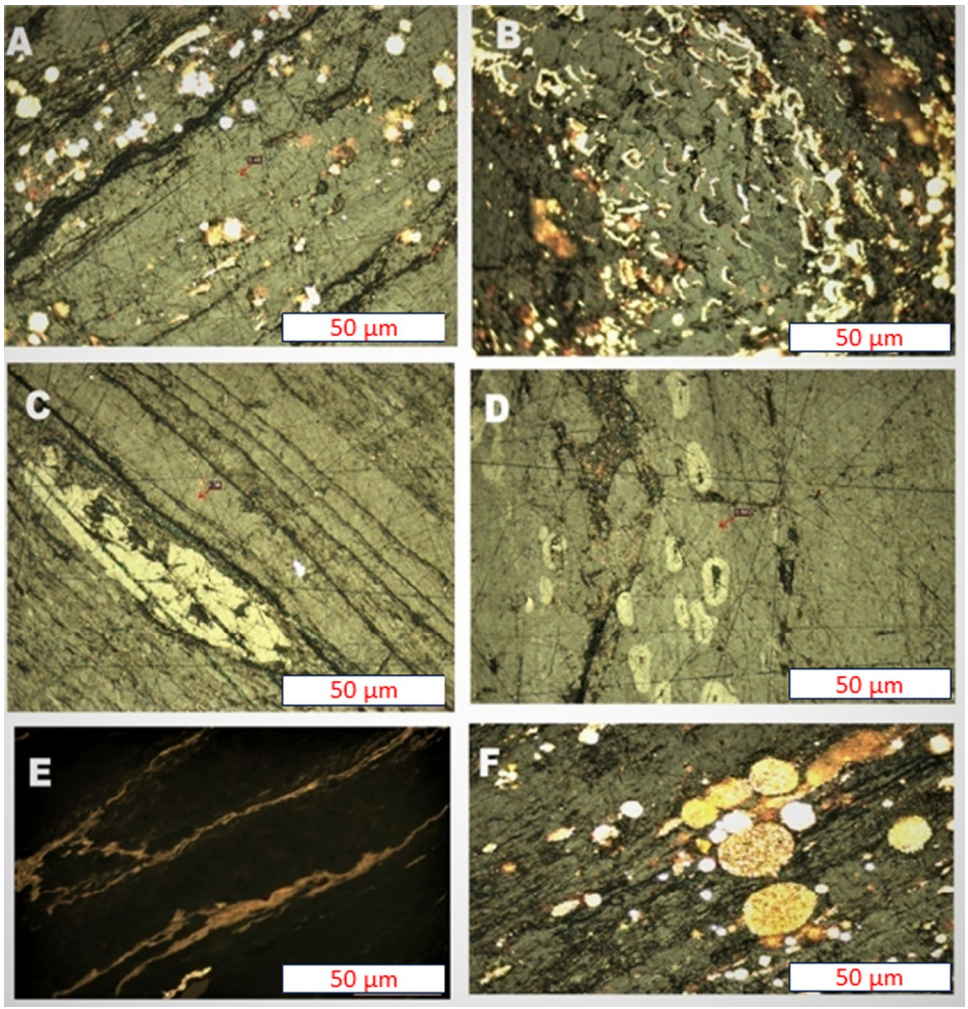

Fig. 1 Representative photomicrographs of macerals of Tirap colliery coals (TPHM1), Makum coalfield: **a** Collotelinite, cutinite, exsudatinite and framboidal pyrite (in white light); **b** Collodetrinite; semifusinitem and pyrite (in white light); **c** Collotelinite, semifusinite, cutinite and sporinite (under white light); **d** Collotelinite and funginite (fungal spore); **e** Exsudatinite, cutinite and liptodetrinite (in fluorscent light); **f** Collodetrinite and framboidal pyrites (in white light)

Inertinite macerals in the Makum coal are represented by semifusinite (Fig. 1b) and funginite (Fig. 1d). Formation of semifusinite is caused by suberial exposure of deposited plant debris in the peat swamp and sometimes by wildfires too (Scott 1989). The collotelinites in the Makum coal shows mean vitrinite reflectance (Vro in oil) around 0.5% indicating subbituminous rank of the coal (Mackowsky et al. 1997). The significant amount of visible mineral matters in the Makum coal are represented by framboidal pyrites (Fig. 1a and b). Seawater interaction with peats in brackish water environment results in an elevated amount of sulphur in coal (Bustin and Lowe 1987). Abundance of pyritic sulfur in the Makum coal thus indicates deposition of the vegetal debris in a coastal/deltaic environment. Certain types of plant material, such as ferns, are more likely to contribute to the formation of liptinite-rich coals (Scott and Collinson 2020). The higher amount of liptinite indicates perhydrous nature of Makum coal. High liptinite content may also make these coal more reactive. Coals with high liptinite content has a higher propensity for spontaneous combustion than coals with low liptinite content which may be due to the presence of easily oxidizable organic matter in the liptinite that can generate heat and lead to spontaneous combustion (Misra and Singh 1994).

3.2 PAAS normalised REEs distribution patterns in the Tirap coal and associated OB/sediments

REE are difficult to fractionate during deposition, and sedimentary REE patterns may reveal significant information about their geochemical evolution (Mclennan 1989). For the current investigation, the REE concentrations in the related sediments and Makum coal samples, are normalised using Post Archean Australian Shale (PAAS), (normalization data after Mclennan 1989) (Tables S5 and S6). The PAAS normalised REE distribution patterns of the studied samples show relative depletion of LREE compared to slight HREE enrichment with a minor bulge at Nd, Sm, Eu, and Gd. These patterns mimic the REE distribution patterns of marine shales (Fig. S3) (Cullers and Podkovyrov 2002). All the samples show slight Ce negative anomaly except sample TPHM2. The total REE ($\sum$REE) content of a coal

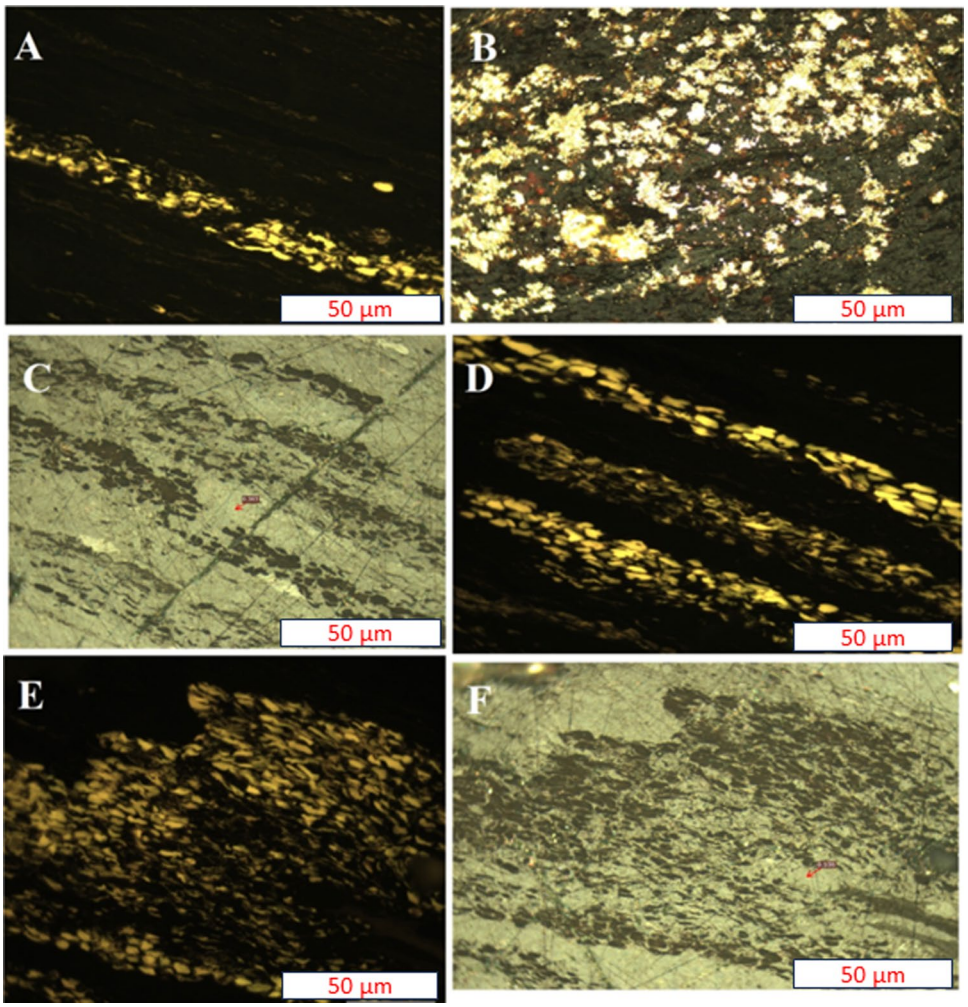

Fig. 2 Representative photomicrographs of macerals of Tirap colliery coals (C3), Makum coalfield: **a** Resinite, liptodetrinite and sporinite (in fluorscent ligth); **b** Collodetrinite and pyrite (in white light); **c** Collotelinite, sporinite and resinite (in white light); **d** Resinite (in fluorscent light); **e** Resinite and collotelinite (in white light)

sample is a measure of their abundance related to geochemical association with either organic matter and/or mineral matter since REE cannot make their own minerals. Studies carried out by Hower et al., (2016) and Zhang et al. (2015) reported the general partioning of HREE. According to their studies, HREEs prefer to associate with organic matter, while LREEs have a greater affinity to associate with the mineral matter in coal. If this is the case, one can argue that low rank coals should inevitably rich with LREE and high rank coal with HREE. But this not the case in general observed (Laudal et al. 2018). In the present case, the coal samples (C1–C3) show extremely low total REE in the range of 19–44 ppm (PAAS 211.77 ppm), whereas the OB and sediment samples show 118–209 (ppm) except TPHM1, 2, and TCP-20 in which the total REE range is comparable to coal samples (37–51 ppm). Y/Ho values range from 23 to 32 (PAAS = 27) and Ce/Ce* (Ce-anomaly) range between 0.02 to 0.10 for coal samples and 0.08 to 2.90 for OB samples which indicate negative anomalies for coals and positive to negative anomalies for OB samples, indicating a mixed environment of oxic to anoxic in nature. OB samples that mimic shaly composition indicate oxic and anoxic conditions are shown by coal samples. Similarly, Eu/Eu* (Eu-anomaly) range between 1.00 to 1.30 (PAAS = 0.21) indicating flat to slight positiveness indicating mild oxic environment. Since the quantities of REE in the sediment samples are lower than those found in PAAS and UCC, it is more likely that spontaneous geological events than human action have been accountable for the distributions of REE in the analysed marine sediment samples (Kritsananuwat et al. 2015). A comparison made between the studied samples (combined coal and OB samples) of the present investigation with important earth reservoirs and source rocks (mafic and felsic) indicate that a mixed provenance (mafic + felsic) is responsible for their deposition and also exhibit a good agreement with Upper Continental Crust (UCC) and Post Archean Average shale (Table S7). These proxies and findings further reflect on the possibility in the future to distinguish from any anthropogenic intrusion in this location. As a result, the knowledge gathered in this study can assist in clarifying the natural concentrations of these components and will be valuable for future environmental monitoring

efforts. (Eu/Eu* and Cc/Ce* are calculated based on Bau and Dulski 1996).

3.3 Physico-chemical characteristics of aqueous coal and OB leachates and residues

Table 1 depicts the results of the physico-chemical parameters, consisting of pH, EC, TDS, DO for the aqueous leachates obtained by performing aqueous leaching experiments of coal (TpC20) and overburden (TpOB20) at various time and temperature junctures. It shows that the pH values of leachates decrease gradually from 30 min of leaching to 90 min of leaching time at temperature of 25, 45, and 90 °C, respectively. The EC of the leachates of the samples at same temperature and different reaction time first increases and then decreases. The dissolved oxygen (DO) of the aqueous leachates decreases at constant temperature and varying reaction time. The acid discharging tendency of the overburden sample TpOB-9(pH 2.4) is found to be more as compared to that of Tirap coal leachate TpC-9(pH 4.5), despite the application of same leaching parameters of 90 °C and 90 min for both coal and overburden samples. Similarly, the TDS, Fe, and SO_4^{2-} concentration values are found to be increased progressively with an increase in the time frame of the leaching process and the temperature of the leaching medium.

3.4 Observations from XPS analysis of aqueous leachate samples

Aqueous leachates of coal (TpC-3) and over burden (TpOB-3), obtained on leaching of coal (TpC20) and OB(TpOB20) for 1 h at room temperature has been analysed for determining the functional groups present along with its binding energy. The XPS spectra of TpC-3 and TpOB-3 are shown in Fig. 3. The deconvoluted XPS spectra of C_{1s} for both the samples (Fig. 3a, b) depicts significant peaks at 283.2 and 287.4 eV correlating to sp^2 C–C, and C-S, respectively. The C-S indicates the possible effect of organic sulfur on the formation of acidic mine-water. The deconvoluted spectra of Fe_{2p}, Fig. 3c and d) shows binding energies at 708.7, 711.4, and 722.2 eV for TpC and at 709.8, 713.1, and 723.4 eV that are attributed to the presence of Fe^{2+} and Fe^{3+}, respectively. The Fe^{2+} and Fe^{3+} ions indicate the presence of FeS_2 and other functional groups possessing ferric ions ($Fe(OH)_3$, FeO (OH), Fe_2O_3). The deconvoluted XPS spectra of S_{2p} for both the coal and OB (Fig. 3e, f) represents the presence of SO_4^{2-} at a binding energy of 167.6 eV. Hence, from the evidence of presence of pyrite and other ferric ions along with the C-S bond in the aqueous leachates of coal and OB samples, generation of AMD can be confirmed.

3.5 Kinetics of aqueous depyritisation

The kinetics of depyritisation of coal in water has been studied extensively. It reveals that the aqueous leaching; for a day time (i.e., 24 h) shows the maximum pyritic sulfur removal of 59.42% at 90 °C, 57.30% at 45 °C, and 52.88% at 25 °C for TpC; and 81.86% at 90 °C, 78.02% at 45 °C, and 74.30% at 25 °C for TpOB samples, respectively (calculated from Table S8). As a result, when the temperature of the environmental reaction systems rises, the amount of pyritic sulfur eliminated by atmospheric aqueous oxidation increases (Baruah et al. 2006). The kinetic parameters of depyritisation of both the samples (Table 2) suggest a pseudo-first-order reaction kinetics (Fig. 4a & b). The following equation is used to calculate the pseudo-first order reaction kinetics:

$$k = 1/t[\ln(C_0 - C_\infty/(C_t - C_\infty]$$

where, C_0, C_t, and C_∞ stand for the concentrations of pyritic sulfur in the coal samples at 0, t, and infinity (say 24 h).

The Arrhenius plots (Fig. 4c and d) based on the rate constants results the activation energies of 3.288 and 2.684 kJ/mol for the depyritisation of coal (TpC) and OB (TpOB) in aqueous media from the slope (Table 2). The intercepts of the plot yield the frequency factors (A) of 0.0902 and 0.0868 min^{-1} for coal and OB, respectively. In this case, it is shown that the rate constants climb as the temperature of the reacting system rises. This is consistent with how a chemical reaction's pace often depends on temperature.

3.6 Results of prototype development and mitigation of AMD water

After running a specific amount of untreated mine water through the burette and stacking them with new limestone, the AMD water turns out to be neutral. Table S9 shows the amounts of mine water necessary for neutralisation in each burette, together with the flow rates, total amount of limestone, pH, and expected time. After running 20 mL of mine water through the burette with different concentrations of limestone, such as 10 g, 20 g, 30 g, and 40 g, the final pH of the mine water is measured to be 6.3, 6.4, 6.5 and 6.6, respectively. Accordingly, at this stage, the mine water has EC values of 5.63, 5.26, 4.98, and 4.71 mS/cm and DO values of 4.59, 4.28, 4.47, and 4.30 mg/L, for 10, 20, 30, 40 g of limestone, respectively (Table S10). The volume of AMD collected adjacent to the mining region determines the amount of limestone to be used in remediation for complete neutralisation (pH 7) and removal of potentially harmful components contained in AMD water. Table S10 shows that the pH gradually changes after the treatment by varying the amount of the limestone used.

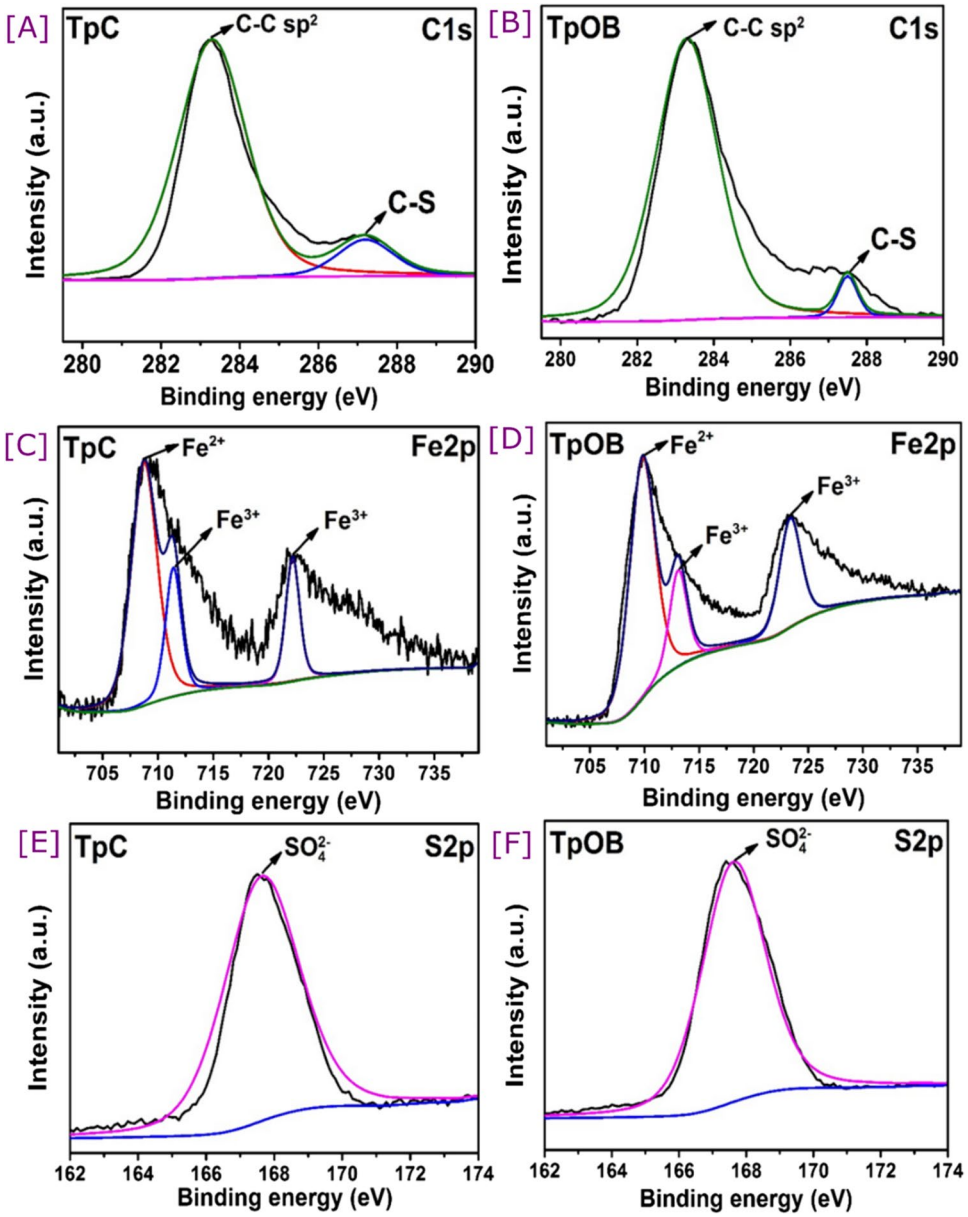

Fig. 3 XPS Deconvoluted spectra of the aqueous leachates of coal (TpC20) for **a** C_{1s} (C) Fe_{2p} and (E) S_{2p}. XPS deconvoluted spectra of the aqueous leachates of coal (TpOB20) for **b** C_{1s} **c** and **d** Fe_{2p} and **e** and **f** S_{2p}

Table 2 Kinetic parameters for aqueous oxidation of pyritic sulfur in Tirap coal and overburden samples

Sample	Temperature (K)	Rate constant (min^{-1})	Activation energy (kJ/mol)	Frequency factor (min^{-1})
TpC20	298	0.0240	3.288	0.0902
	318	0.0249		
	363	0.0308		
TpOB20	298	0.0280	2.684	0.0868
	318	0.0325		
	363	0.0353		

We noticed a change in the pH of the AMD water from the typical acidic (2.9–3.1) pH after the aforementioned series of treatment process undergone in the prototype station as displayed in Table S11. A total of 1000 L of AMD water was used across the three AMD treatment batches in two phases. After the first batch of processing, we notice that the pH has increased to 6.1. The pH value at 6.7 and 6.4, respectively, is the greatest at the end of the second and third batch. It's feasible that the limestone dissolves in the acidic water, raising the pH and imparting alkalinity. According to a number of previous research, limestone could potentially use as a feasible

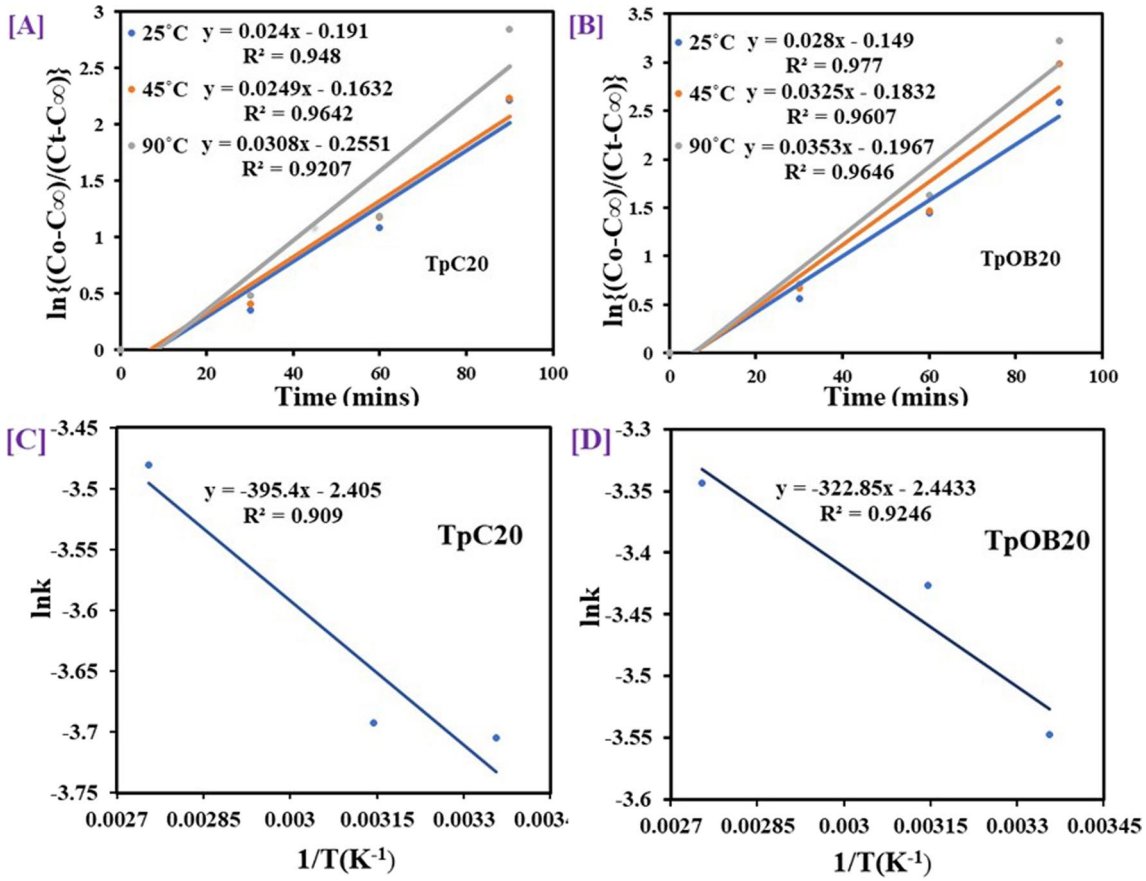

Fig. 4 **a** Pseudo-unimolecular kinetic plot for pyritic sulfur oxidation of coal (TpC20) and **b** Oover burden (TpOB20) samples at different times, **c** Arrhenius plot for the aqueous pyritic sulfur oxidation in coal (TpC20) and **d** over burden (TpOB20) samples

alternative to effectively remove metals from industrial waste water, since it has high metal binding characteristics for ions and elements (such as heavy metals) (Ma et al. 2012). The adsorption capacity of $CaCO_3$, in limestone is stated to be greater in the current study due to variability in the abilities of metal sorption and adsorption affinity of $CaCO_3$ (Arakaki and Mucci 1995; Ma et al. 2012). In addition to neutralising the metals, this procedure aids in reducing the concentration of heavy metals, which are tend to accumulate in AMD.

3.7 Mechanism of AMD treatment

AMD is common in coal overburden where the carbonate minerals calcite ($CaCO_3$) and dolomite ($CaMg(CO_3)_2$) are absent or deficient relative to pyrite (Vogel 1961). The following processes can be used to enhance pH, alkalinity ($HCO^{3-} + OH^-$), and Ca^{2+} concentrations in mine water via the dissolving of calcite, the primary component of limestone:

$$CaCO_3(s) + 2H^+ \longrightarrow Ca^{2+} + H_2CO_3 \quad (4)$$

$$CaCO_3(s) + H_2CO_3 \longrightarrow Ca^{2+} + 2\,HCO_3^- \quad (5)$$

$$CaCO_3 + H_2O \longrightarrow Ca^{2+} + HCO_3^- + OH^- \quad (6)$$

where, $H_2CO_3 = CO_2$ (aq) H_2CO_3 (Plummer et al. 1979; Stumm and Morgan 1996) The rate of calcite dissolution is affected by pH, CO_2 partial pressure (PCO_2), and the activities of H_2O, Ca^{2+}, HCO_3^- and near the calcite surface (Plummer et al. 1979; Xue et al. 2009). The reaction between AMD and limestone that takes place during remediation is as follows:

$$CaCO_3 + 2H^+ + SO_4^{2-} \longrightarrow Ca^{2+} + SO_4^{2-} + H_2O + CO_2 \quad (7)$$

Through a reaction with limestone, the H_2SO_4 in AMD releases Ca^{2+} into the treated AMD. AMD is continuously

passed through limestone, which causes a rise in $CaCO_3$ consumption and a decrease in H^+ ion concentrations (by raising pH). The process terminates when the pH of the treated AMD reaches 7 after a specified period of time. Compared to other elements, Pb has a stronger affinity for limestone. (Dutta et al. 2020; Plummer et al. 1979). Limestone has the ability to bind considerable amounts of Cu and Fe from mine water on its surface, with the ability of binding in the following order: Cu > Fe > Zn > Ni (Iakovleva et al. 2015).

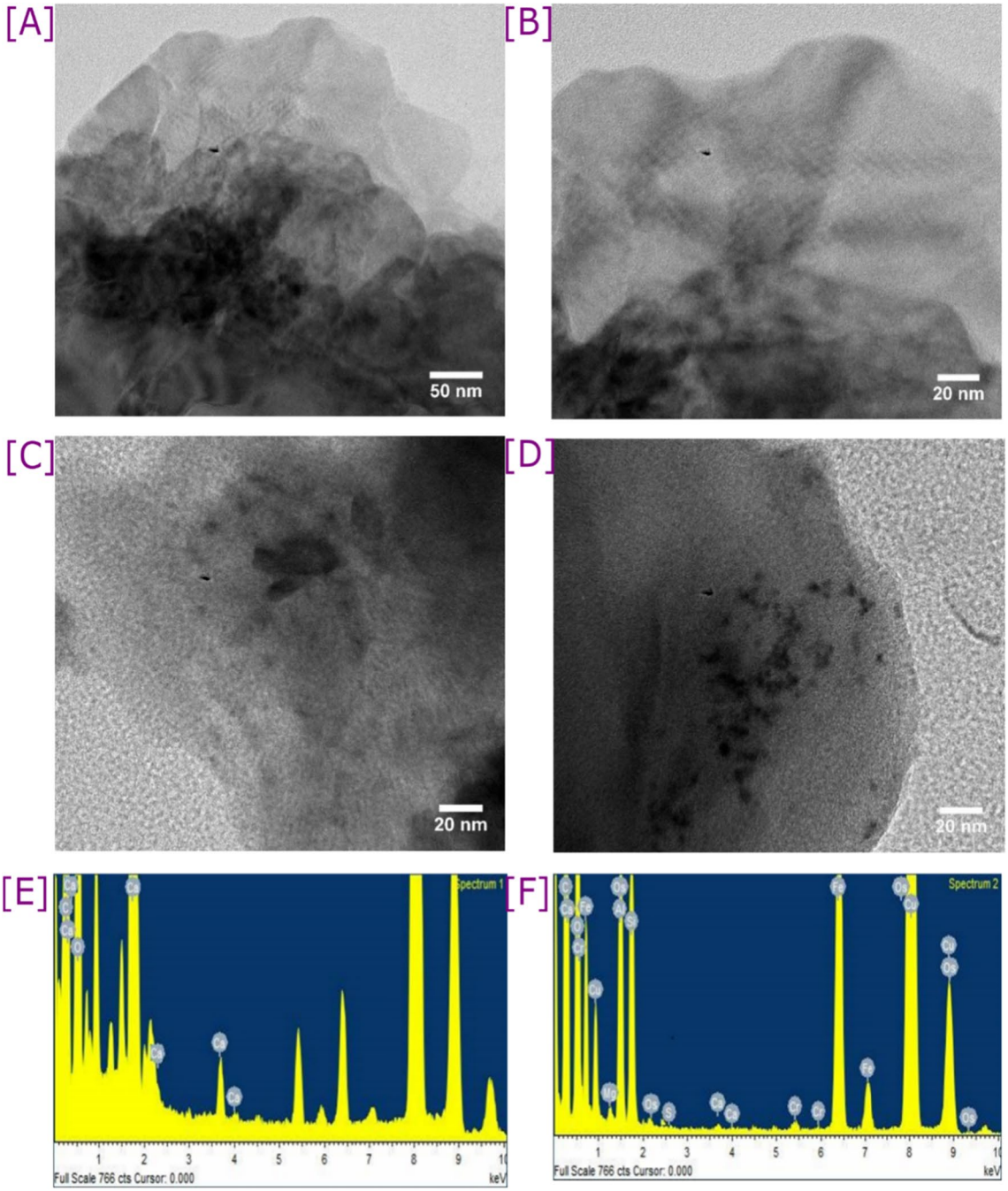

Fig. 5 HRTEM images showing the limestone before the treatment of AMD indicating the presence of calcite nanoparticles in limestone (**a**, **b**); the limestone particles after the treatment of AMD (**c**, **d**); The EDS image of limestone before (**e**) and after (**f**) treatment of AMD water indicating the absorption of elements present in AMD water

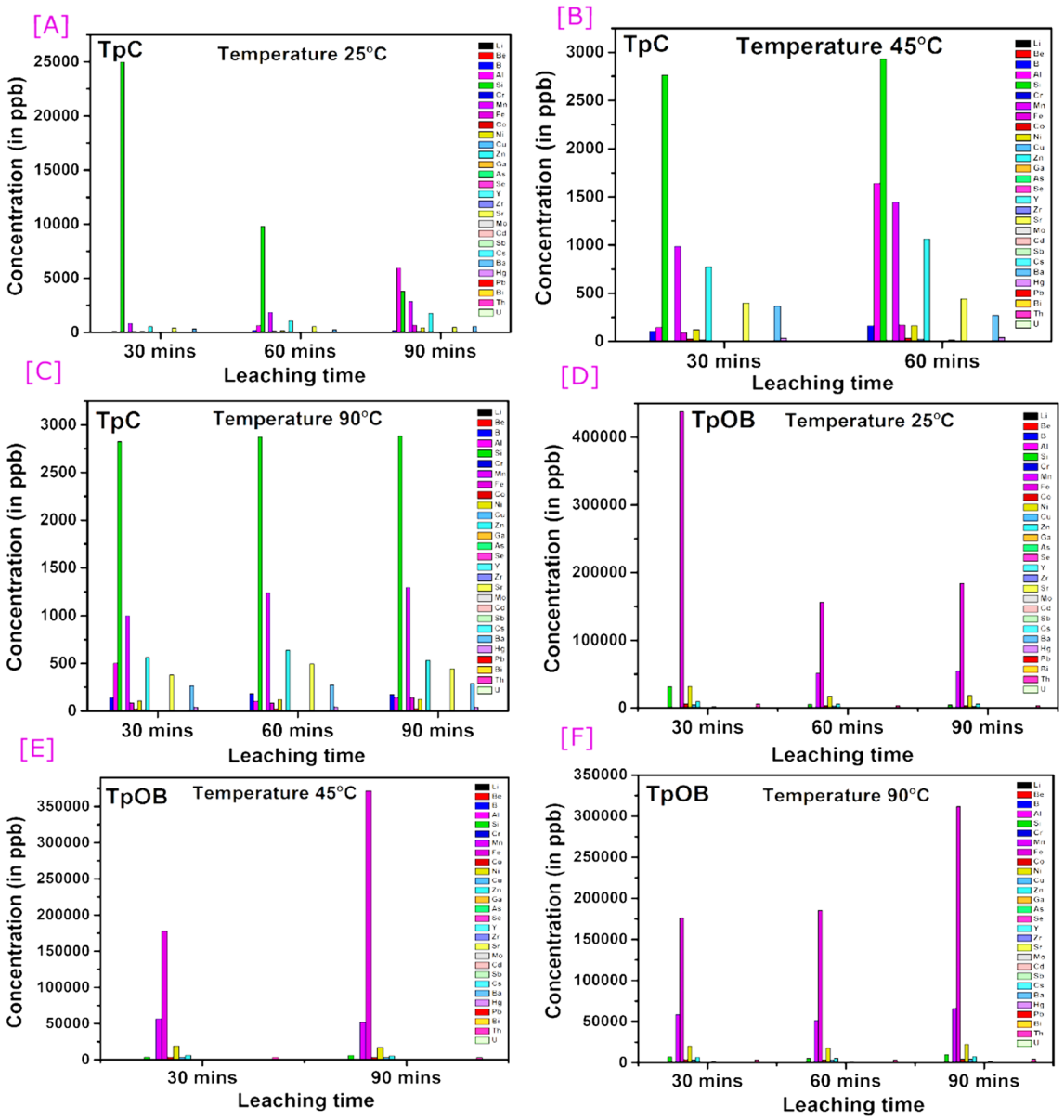

Fig. 6 ICP-OES analysis showing change in elemental concentration (in ppb) in aqueous leachates of **a** Tirap coal (TpC20) with leaching time (in min) at 25 °C, **b** Tirap coal (TpC20) with leaching time (in min) at 45 °C, **c** Tirap coal (TpC20) with leaching time (in min) at 90 °C, **d** Tirap over burden (TpOB20) with leaching time (in min) at 25 °C, **e** Tirap over burden (TpOB20) with leaching time (in min) at 45 °C, **f** Tirap over burden (TpOB20) with leaching time (in min) at 90 °C

3.8 Observations from TEM/HRTEM analysis of limestone before and after the treatment

From TEM/HRTEM analysis, it is found that some fraction of Meghalaya limestone reveals the presence of $CaCO_3$ particles (Fig. 5a, b). Figure 5c, d also shows the limestone particles after being treated with mine water. The Energy Dispersive Spectroscopy (EDS) of the treated limestone particles confirms the presence of C, Ca, Fe, Os, Cr, O, Cu, Mg, Al, Si, and S, indicating the absorption of contaminants from AMD water (see Fig. 5e, f). In contrast, untreated limestone only contains Ca, C, and O, thereby indicating the effect of limestone in mitigating AMD.

3.9 ICP-OES analysis of elements

3.9.1 ICP-OES analysis of aqueous leachates of coal, OB and mine water

ICP-OES analysis of aqueous leachates of TpC20 and TpOB20 have been performed to ascertain the effects of temperature and reaction time on the elemental concentrations.

The ICP-OES analysis of the aqueous leachates of the TpC20 and TpOB20 performed at (30, 60, 90 min) and temperature (i.e., at 25, 45, 90 °C) reveal that the concentration of different elements like Al, Ba, Co, Ni, Fe, Mn, Cu, Cr and Zn increase with leaching time and temperature. From Fig. 6a, b, c, it is observed that the aqueous leachates of TpC20 contain the major elements like Al, Fe, Mn, Ba, Cr, Co, Ni, Zn, Cu, Pb, etc., along with some other minor elements with a rise in concentrations on increasing leaching time (i.e., at 30, 60, 90 min) and temperature (i.e., at 25, 45, 90 °C). However, for the aqueous leachates of TpOB20 [see Fig. 6d, e, f], a number of anomalies are observed at different temperatures (25 and 45 °C) and with increase in leaching time. While for the aqueous leachates of TpOB20 at reaction temperature of 90 °C, with increase in leaching time, most of the elements like Si, Fe, Mn, Cr, Co, Ni, Zn, and Cu are observed to be release more in water. The concentrations of Cd, Pb, Hg and Se are found in low concentrations in all the aqueous leachates. At high temperature most of the elements are leached from coal and over burden samples even at a short leaching time. Thus, from the above observations, it can be stated that most of the major elements including trace/hazardous elements are released from the coal and over burden samples with increase in reaction time and temperature.

3.9.2 ICP-OES analysis of treated mine water samples collected from the prototype unit

ICP-OES analysis of treated mine water samples are performed to detect the overall change in elemental concentrations on remediation utilising a variety of techniques. The data for both the two sets of the limestone and water hyacinth (distinguished as set A and B) is mentioned in Table S12 and S13 and the result shows a quite promising repetitive pattern. It is discovered that the concentration of components Al, B, Ca, and Cd follows a declining pattern on treatment of the AMD water. The results are showing almost a regular decreasing trend from S1 stage to S3 stage in the elemental concentration of Al, B, Cu, Fe, and Ni for all the four sets of samples i.e., (S1R1, S2R1, S3R1), (S1R2, S2R2, S3R2), (S1R3, S2R3, S3R3) and (S1R4, S2R4, S3R4) collected after passage of R1, R2, R3, R4 amount of water in four different runs, respectively. Moreover, complete elimination of Pb, Zn and Cd has been observed for both phase A and phase B samples from Table S12 and S13. It is assumed that, minimization or complete elimination of elements, heavy metals from the AMD water can be done by adapting this remediation method in a large scale. Limestone revealed a good binding capability for elements such as heavy metal. Moreover, limestone is a very good adsorbent also. In addition of neutralising the metals, this procedure aids in reducing the concentration of heavy metals, which are typically present in AMD. This ICP-OES research revealed that the concentrations of the majority of the components detected in AMD water decrease as the water flows through the limestone. In the remediation process, the limestone has been used as an absorbent for removing some representative metals found to be present in AMD water from the Tirap colliery. In the case of Cu, Co, Zn, Fe, and Ni, the removal is almost completed when passed through limestone having particle size of 0.003180 m.

4 Conclusions

During the monsoon season, AMD produce by the coal mining activities in Northeast India is a major source of toxic elements and ions in the nearby water system. Aqueous leaching of Tirap coal and overburden samples, performed at various temperatures and time regimes reveals that the oxidation of pyrite (Depyritisation) follows a pseudo-first order reaction kinetics. The physico-chemical characteristics of the samples are examined using modern experimental instruments and laboratory-based techniques. The physico-chemical analysis of aqueous coal leachates reveals that there is a very weak co-relation between pH, EC and TDS of mine water. But, there is a substantial link between EC and TDS in mine water. The high TDS value of the leachates and AMD water samples originated from mining prone region cause the dissolution of a significant number of ions in soil, which spread into water bodies and neighbouring land along with AMD water. To accomplish ecologically sound and sustainable mining adopting a suitable strategy for management based on AMD's biogeochemical properties is vital. We have demonstrated two distinct AMD remediation techniques, one in a lab and the other in a prototype station. The limestone is employed as an absorbent to remove some of the representative metals found in AMD water from the Tirap colliery. Untreated limestone has Ca, C, and O, whereas treated limestone contains C, Ca, Fe, Os, Cr, O, Cu, Mg, Al, Si, and other elements. The results of the ICP-OES study suggests that the concentrations of majority of the elements present in AMD water drop after passing through the limestone. The consumption of $CaCO_3$ increases with the continuous passage of AMD through limestone, while the concentration of H^+ ions decrease (by raising pH). After a certain period of time, the pH of the treated AMD reaches almost 7.0 and the reaction terminates. By adjusting the amount of limestone used, the pH, EC, and DO values progressively alter after treatment. The prototype produced for the treatment is used to process AMD in three steps. We have found that the pH increase to 6.1 after the first round of processing. The pH value is highest near the conclusion of the second and third batches, at 6.7 and 6.4, respectively. The total outcomes of the experiment may indicate a feasible method for mitigating the problem of acid mine drainage in a more environmentally conscious and sustainable manner.

Hence, in this study we have demonstrated a detailed procedure of how acidic water is consequently mitigated and lessened through holistic evaluation of AMD from its genesis and through disposal of waste materials. As a future scope, technological advances in process equipment, cutting-edge research and development for AMD mitigation treatment and retrieval of resources have a lot of room for growth. Assessing the quality of the OB, rock garbage dumps, mining waste, and monitoring of AMD, can assist in anticipating emergent issues, developing effective treatment projects, and revitalising the mine sites for utilization in the future. On this groundwork, a further discussion of AMD's resource utilization status and significance is to be undertaken.

Supplementary Information The online version contains supplementary material available at https://doi.org/10.1007/s40789-023-00658-6.

Acknowledgements Authors express thanks to the Director, CSIR-NEIST for the permission to conduct the study. The financial grant (GPP364) received from Ministry of Earth Science (MoES), Govt. of India is thankfully acknowledged. Authors are thankful to the OIL, Guwahati for petrographic analysis. Authors express the esteemed reviewers for their constructive comments to revise the draft.

Declarations

Conflict of Interest The authors declare that they have no known competing financial interests or personal relationships that could have appeared to influence the work reported in this paper.

References

Arakaki T, Mucci A (1995) A continuous and mechanistic representation of calcite reaction-controlled kinetics in dilute solutions at 25 C and 1 atm total pressure. Aquat Geochem 1:105–130

ASTM D (2013) Standard Practice for preparing coal samples for analysis, West Conshohocken, PA, 19428-2959 USA

ASTM D 2492 – 02: Standard Test Method for Forms of Sulfur in Coal, West Conshohocken, PA, 19428-2959 USA

Ayora C, Macías F, Torres E, Lozano A, Carrero S, Nieto J-M, Pérez-López R, Fernández-Martínez A, Castillo-Michel H (2016) Recovery of rare earth elements and yttrium from passive-remediation systems of acid mine drainage. Environ Sci Technol 50:8255–8262

Baruah BP, Saikia BK, Kotoky P, Rao PG (2006) Aqueous leaching on high sulfur sub-bituminous coals, in Assam, India. Energy Fuels 20:1550–1555

Bau M, Dulski P (1996) Distribution of yttrium and rare earth elements in the Penge and Kuruman iron formation. Transvaal Supergroup South Africa Precambrian Res 79:37–55

Binnemans K, Jones PT, Blanpain B, Van Gerven T, Yang Y, Walton A, Buchert M (2013) Recycling of rare earths: a critical review. J Clean Prod 51:1–22

Bustin R, Lowe L (1987) Sulphur, low temperature ash and minor elements in humid–temperate peat of the Fraser River Delta, British Columbia. J Geol Soc 144:435–450

Chabukdhara M, Singh O (2016) Coal mining in northeast India: an overview of environmental issues and treatment approaches. Int J Coal Sci Technol 3:87–96

Chen G, Ye Y, Yao N, Hu N, Zhang J, Huang Y (2021) A critical review of prevention, treatment, reuse, and resource recovery from acid mine drainage. J Clean Prod 329:129666

Chon HT, Kim JY, Choi SY (1999) Hydrogeochemical characteristics of acid mine drainage around the abandoned Youngdong coal mine in Korea. Resour Geol 49:113–120

for Coal, I.C. (2001) The new inertinite classification (ICCP System 1994). Fuel 80:459–471

Cullers RL, Podkovyrov VN (2002) The source and origin of terrigenous sedimentary rocks in the Mesoproterozoic Ui group, southeastern Russia. Precambr Res 117:157–183

Daraz U, Li Y, Ahmad I, Iqbal R, Ditta A (2022) Remediation technologies for acid mine drainage: Recent trends and future perspectives. Chemosphere 137089.

Du T, Bogush A, Mašek O, Purton S, Campos LC (2022) Algae, biochar and bacteria for acid mine drainage (AMD) remediation: a review. Chemosphere 304:135284

Dutta M, Islam N, Rabha S, Narzary B, Bordoloi M, Saikia D, Silva LF, Saikia BK (2020) Acid mine drainage in an Indian high-sulfur coal mining area: cytotoxicity assay and remediation study. J Hazard Mater 389:121851

Gogoi M, Kumar TS, Phukan S (2020) Organic geochemistry, petrography, depositional environment and hydrocarbon potential of the Eocene coal deposits of west Daranggiri Coalfield, Meghalaya. J Geol Soc India 95:84–94

Hower JC, Granite EJ, Mayfield DB, Lewis AS, Finkelman RB (2016) Notes on contributions to the science of rare earth element enrichment in coal and coal combustion byproducts. Minerals 6:32

Humphries M (2010) Rare earth elements: the global supply chain. Diane Publishing

Iakovleva E, Mäkilä E, Salonen J, Sitarz M, Wang S, Sillanpää M (2015) Acid mine drainage (AMD) treatment: neutralization and toxic elements removal with unmodified and modified limestone. Ecol Eng 81:30–40

ICCP (1998) The new vitrinite classification (ICCP System 1994). Fuel 77:349–358

Ighalo JO, Kurniawan SB, Iwuozor KO, Aniagor CO, Ajala OJ, Oba SN, Iwuchukwu FU, Ahmadi S, Igwegbe CA (2022) A review of treatment technologies for the mitigation of the toxic environmental effects of acid mine drainage (AMD). Process Saf Environ Prot 157:37–58

Jiao Y, Zhang C, Su P, Tang Y, Huang Z, Ma T (2023) A review of acid mine drainage: Formation mechanism, treatment technology, typical engineering cases and resource utilization. Process Safety Environ Protect

Kritsananuwat R, Sahoo SK, Fukushi M, Chanyotha S (2015) Distribution of rare earth elements, thorium and uranium in Gulf of Thailand's sediments. Environ Earth Sci 73:3361–3374

Laudal DA, Benson SA, Palo D, Addleman RS (2018) Rare earth elements in North Dakota lignite coal and lignite-related materials. J Energy Res Technol 140:062205

Li X, Wu P (2017) Geochemical characteristics of dissolved rare earth elements in acid mine drainage from abandoned high-As

coal mining area, southwestern China. Environ Sci Pollut Res 24:20540–20555
Ma X, Li L, Yang L, Su C, Wang K, Yuan S, Zhou J (2012) Adsorption of heavy metal ions using hierarchical CaCO3–maltose meso/macroporous hybrid materials: adsorption isotherms and kinetic studies. J Hazard Mater 209:467–477
Mackowsky MT, Teichmuller M, Taylor G, Chandra D, Teichmuller R, Bwnfraeger G, Berlin S, Cloth D, Hacquebard PA, Darfmoufh, NS (1997) Stach's textbook of coal petrology. Gebruder borntraeger
Martínez NM, Basallote MD, Meyer A, Cánovas CR, Macías F, Schneider P (2019) Life cycle assessment of a passive remediation system for acid mine drainage: towards more sustainable mining activity. J Clean Prod 211:1100–1111
Mathur L, Evans P (1964) Oil in India: 22nd session international geological congress proceedings. New Delhi
Mclennan SM (1989) Rare earth elements in sedimentary rocks; influence of provenance and sedimentary processes. Rev Mineral Geochem 21:169–200
Misra BK, Singh BD (1994) Susceptibility to spontaneous combustion of Indian coals and lignites: an organic petrographic autopsy. Int J Coal Geol 25:265–286
Misra BK (1990) Tertiary coals of Makum Coalfield, Assam, India: Petrography, genesis and sedimentation
Pickel W, Kus J, Flores D, Kalaitzidis S, Christanis K, Cardott B, Misz-Kennan M, Rodrigues S, Hentschel A, Hamor-Vido M (2017) Classification of liptinite–ICCP System 1994. Int J Coal Geol 169:40–61
Plummer L, Parkhurst D, Wigley T (1979) Critical review of the kinetics of calcite dissolution and precipitation
Saikia BK, Ward CR, Oliveira ML, Hower JC, De Leao F, Johnston MN, O'Bryan A, Sharma A, Baruah BP, Silva LF (2015b) Geochemistry and nano-mineralogy of feed coals, mine overburden, and coal-derived fly ashes from Assam (North-east India): a multifaceted analytical approach. Int J Coal Geol 137:19–37
Saikia B, Saikia A, Baruah B (2015a) Nature and chemistry of coal and its products. Coal Production and Processing Technology, CRC Press, Boca Raton, USA, pp 3–30
Scott AC (1989) Observations on the nature and origin of fusain. Int J Coal Geol 12:443–475
Scott AC, Collinson ME (2020) A note on the charring of spores and implications for coal petrographic analysis and maceral nomenclature. Int J Coal Geol 219:103361
Singh MP, Singh AK (2001) Source rock characteristics and maturation of Palaeogene coals, Northeast India. Geol Soc India 57:353–368
Stumm W, Morgan JJ (1996) Aquatic chemistry chemical equilibria and rates in natural waters
Sun H, Chen M, Zou L, Shu R, Ruan R (2015) Study of the kinetics of pyrite oxidation under controlled redox potential. Hydrometallurgy 155:13–19
Swer S, Singh O (2004) Status of water quality in coal mining areas of Meghalaya, India. In: Proceedings of the national seminar on environmental engineering with special emphasis on mining environment, pp 19–20
Tu Z, Wu Q, He H, Zhou S, Liu J, He H, Liu C, Dang Z, Reinfelder JR (2022) Reduction of acid mine drainage by passivation of pyrite surfaces: a review. Sci Total Environ 832:155116
Villegas-Plazas M, Sanabria J, Arbeli Z, Vasquez Y, Roldan F, Junca H (2022) Metagenomic analysis of biochemical passive reactors during acid mine drainage bioremediation reveals key co-selected metabolic functions. Microbial Ecol, pp 1–8
Vogel AI (1961) A text-book of quantitative inorganic analysis, including elementary instrumental analysis. (No Title)
Xue Y, Hou H, Zhu S (2009) Competitive adsorption of copper (II), cadmium (II), lead (II) and zinc (II) onto basic oxygen furnace slag. J Hazard Mater 162:391–401
Zhang W, Rezaee M, Bhagavatula A, Li Y, Groppo J, Honaker R (2015) A review of the occurrence and promising recovery methods of rare earth elements from coal and coal by-products. Int J Coal Prep Util 35:295–330